

MoLA: Motion Generation and Editing with Latent Diffusion Enhanced by Adversarial Training

Kengo Uchida

Sony AI

Tokyo, Japan

kengo.uchida@sony.com

Takashi Shibuya

Sony AI

Tokyo, Japan

takashi.tak.shibuya@sony.com

Yuhta Takida

Sony AI

Tokyo, Japan

yuta.takida@sony.com

Naoki Murata

Sony AI

Tokyo, Japan

naoki.murata@sony.com

Shusuke Takahashi

Sony Group Corporation

Tokyo, Japan

shusuke.takahashi@sony.com

Yuki Mitsufuji

Sony AI, Sony Group Corporation

NY, USA

yuhki.mitsufuji@sony.com

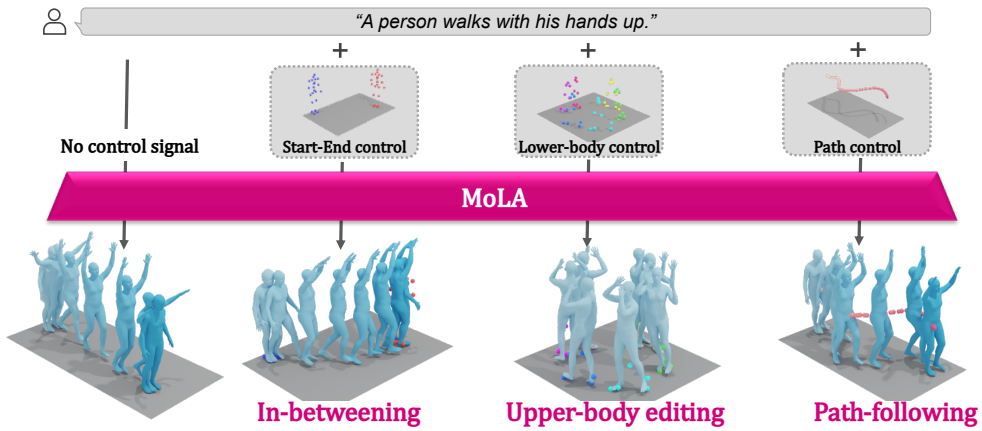


Figure 1: MoLA achieves fast and high-quality human motion generation given textual descriptions while enabling motion editing applications. With MoLA, we can deal with various types of motion editing tasks in a single framework. The above images show the standard text-to-motion generation (as a no-control input case) and three motion editing tasks (with control inputs): the control input for the start-end positions and motion in-between task (left), for the lower body positions and upper body editing task (center), for the motion trajectory and path-following generation task (right).

ABSTRACT

In motion generation, controllability as well as generation quality and speed is becoming more and more important. There are various motion editing tasks, such as *in-betweening*, *upper body editing*, and *path-following*, but existing methods perform motion editing with a data-space diffusion model, which is slow in inference compared to a latent diffusion model. In this paper, we propose MoLA, which provides fast and high-quality motion generation and also can deal with multiple editing tasks in a single framework. For high-quality and fast generation, we employ a variational autoencoder and latent diffusion model, and improve the performance with adversarial training. In addition, we apply a training-free guided generation framework to achieve various editing tasks with motion control inputs. We quantitatively show the effectiveness of adversarial learning in text-to-motion generation, and demonstrate the applicability of our editing framework to multiple editing tasks in the motion domain. We will make our code publicly available.

CCS CONCEPTS

- Computing methodologies → Computer vision; Motion processing.

KEYWORDS

Motion generation, Latent diffusion model, Adversarial training, Guided generation

1 INTRODUCTION

Motion generation is a fundamental task in multimedia production and computer animation, and it can be challenging due to the diversity of possible motions and the difficulty and cost of obtaining high-quality data. Generating human motions from textual descriptions, i.e., text-to-motion generation, is an emerging task that may play an important role in a broad range of applications such as games, film, the metaverse, and virtual reality. Over the past few years, text-to-motion has generated intensive research interest [5, 13, 26, 35, 49, 51, 56, 58, 59]. The existing methods of text-to-motion encompass several different approaches. For example,

| | Fast generation | High-quality generation | Training-free editing |
|------------------------------------|-----------------|-------------------------|-----------------------|
| MDM-based methods [20, 21, 49, 53] | - | - | ✓ |
| Motion Latent Diffusion (MLD) [5] | ✓ | - | - |
| VQ-based methods [13, 26, 35, 56] | ✓ | ✓ | - [†] |
| MoLA (ours) | ✓ | ✓ | ✓ |

Table 1: Comparison of three properties satisfied by MoLA and other text-to-motion methods. [†] Some editing tasks can be done in a training-free manner, but there are editing tasks that cannot be done.

some utilize vector quantization and have achieved high generation performance [13, 26, 35, 56]. Inspired by the development of diffusion models and their convenience, several diffusion-based text-to-motion methods have also been developed to not only generate motion but also to perform editing of the motion samples [49, 58]. In addition, Chen *et al.* adopted a latent diffusion model [39] to enable fast motion generation [5]. Alternatively, other methods for motion editing tasks utilize a pre-trained text-to-motion model as a generative prior, which has attached attention due to its applicability [20, 21, 45, 53].

Ideally, (text-to-)motion generation models should be able to 1) perform fast generation, 2) achieve a high generation performance, and 3) perform editing motions. However, it is difficult for the existing approaches to meet all three requirements. The VQ-based text-to-motion methods [13, 26, 35, 56] require additional training for each editing task, as discussed in [35]. In other words, the VQ-based methods cannot control arbitrary joints in a training-free manner. Requiring extra training per editing task harms the applicability of motion generation models to production. Existing motion editing methods [20, 21, 45, 53] utilize diffusion-based methods in the data-space, such as Motion Diffusion Model (MDM) [49], as a generative prior, but the generation speed of diffusion in the data-space is not fast. In contrast, the existing latent diffusion-based motion generation method [5] performs fast generation, but motion editing based on continuous latent diffusion has not been explored yet.

In this paper, we aim to develop a text-to-motion model that achieves 1) fast generation, 2) a high generation performance, and 3) multiple motion editing in a training-free manner. We summarize the target properties satisfied by our model in Table 1 in comparison with the existing text-to-motion studies. To achieve this goal, we employ a motion variational autoencoder (VAE) to learn a low-dimensional latent representation for diverse human motion sequences and a latent diffusion model using text condition as in [5]. Here, we combine a motion VAE with adversarial training to achieve better reconstruction/generation. It has been verified that adversarial training improves the performance of VAE in the image and audio domains [9, 18, 25, 39], but not yet in motion generation. To the best of our knowledge, our model is the first latent-space motion generation model featuring a VAE is trained with adversarial training. In addition, we introduce training-free guided diffusion [16] into diffusion sampling on latent space to enable multiple motion editing tasks. We empirically show that adversarial training increases the quality on two widely utilized datasets. We also demonstrate that training-free guided diffusion can enable multiple motion editing tasks such as in-betweening, upper body editing, and path-following.

The main contributions of this paper are as follows:

- We propose a new text-to-motion model that can perform fast and high-quality generation and can deal with various types of motion editing tasks (motion in-betweening, upper body editing, and path following) in a training-free manner. To the best of our knowledge, this is the first study to demonstrate motion editing with latent diffusion.
- We quantitatively show that introducing adversarial training to a motion VAE improves reconstruction and generation performance on text-to-motion. To the best of our knowledge, this is the first latent-space motion generation model that introduces adversarial training.

2 RELATED WORK

2.1 Deep Generative Modeling

The progress in generative modeling has developed rapidly over the past decade [11, 22, 42]. In recent years, diffusion models have been actively explored, particularly in the image domain. They have achieved state-of-the-art performance not only in image generation [10, 31] but also in advanced generative tasks such as text-to-image [37, 39, 41], image inpainting [27, 52], and guided generation [54, 57]. A key approach for reducing inference costs is to reduce the essential dimensionality of the target data by learning its compressed representation [10, 39]. This approach involves two stages: learning a VAE to acquire latent representations and then training a diffusion model on the low-dimensional representations.

A pioneering work that incorporates such a two-stage training scheme into generative modeling is VQ-VAE, which aims to compress the target data in a discrete manner [50]. Several subsequent works have followed and expanded this discrete approach [9, 24, 38]. Esser *et al.* attempted to improve the reconstruction fidelity of VQ-VAE through adversarial training [9], which has been adopted by many subsequent works [3, 4, 12, 24]. As another advancement in the stage 1 model, Lee *et al.* generalized the VQ operation to residual vector quantization (RVQ), precisely approximating the encoded feature as a sequence of code stacks [24]. In contrast, VQ-Diffusion adopts a discrete diffusion model that allows the input of a text prompt for learning the discrete latent, thereby achieving text-to-image generation [12]. Mask-prediction training schemes with confidence-based iterative decoding have been proposed for the stage 2 [3, 4].

2.2 Training-free Guided Generation

Starting with works such as [30, 46], there have been many attempts to utilize pre-trained diffusion models as rich priors for various conditional generation tasks without additional training (i.e., *training-free*) [6, 44, 45, 52]. The fundamental idea behind these approaches is to guide the intermediate samples of the diffusion

model during the generation so that the final generated output satisfies the given conditions.

With increasing attention on the practical usefulness of latent diffusion models (LDMs), some recent works have focused on methods capable of dealing with LDMs. FreeDoM [54] performs a variety of conditional generation tasks in a unified framework by designing a task-specific loss function and utilizing the loss during guided sampling. Approaches such as PSLD [40] and MPGDL [16] are attempting to improve on this even more, achieving higher performance and faster guided generation.

2.3 Motion Generation

Text-to-motion generation technology has made rapid progress with the development of neural networks [1, 14, 33, 34, 48]. In particular, diffusion models and VQ-based models have significantly advanced the field of motion generation.

MDM [49] and MotionDiffuse [58] adopt diffusion models for motion generation, which leads to better performance in terms of generation quality. However, these methods directly apply diffusion processes to raw motion sequences, thus resulting in slow generation. MLD [5] mitigates this issue by adopting a diffusion model in a low-dimensional latent space provided by a VAE trained on motion data, inspired by latent diffusion models [39].

VQ-based models have been studied as well, inspired by the success of VQ-based models in image generation [3, 12, 55]. In this approach, a VQ-VAE model is first trained on motion data to acquire discrete motion representations, and deep generative models are then applied to generate sequences of discrete representations (also called tokens). T2M-GPT [56], AttT2M [59], and MotionGPT [19] utilize autoregressive (AR) models to generate motion tokens. However, AR models are slow in inference because motion tokens are generated sequentially. To address this issue, M2DM [23] and DiverseMotion [26] apply discrete diffusion models to motion tokens in a latent space, whereas MMM [35] adopts a mask prediction model. In another line of research, MoMask [13] leverages the RVQ technique to reduce errors caused by the VQ process.

In this paper, we adopt a continuous diffusion model to perform multiple editing tasks with a single framework (Section 3.4). To achieve high-fidelity and fast generation, we boost the performance of a VAE model with adversarial training and apply a diffusion model in the latent space provided by the trained VAE.

2.4 Motion Editing

Motion editing has attracted much research interest as well. MDM [49] demonstrated upper body editing and motion in-betweening by applying diffusion inpainting to motion data in both the spatial and temporal domains. LGD [45] demonstrated path-following motion generation with a guided diffusion that utilizes multiple samples from a suitable distribution to reduce bias. GMD [21] guides the position of the root joint to control motion trajectories. OmniControl [53] controls any joints at any time by guiding a pre-trained motion diffusion model with an analytic function. DNO [20] optimizes the diffusion latent noise of a pre-trained text-to-motion model with user-provided criteria in the motion space and achieves multiple editing tasks. However, these methods employ data-space diffusion models similar to MDM and have not been demonstrated

with a latent diffusion model. Recently, MMM [35] demonstrated motion editing by placing masked tokens in the place that needs editing and applying the mask prediction framework. However, it cannot control an arbitrary body part without additional model training, and the authors trained separate upper-body and lower-body generative models to perform upper-body editing.

In this paper, we employ a latent diffusion model to achieve fast generation and apply a training-free guided generation framework that can deal with multiple editing tasks without additional model training.

3 METHOD

3.1 Overall Framework of MoLA

The goal of this study is to develop a framework for fast and high-quality text-guided motion generation and to deal with multiple control tasks in a training-free way. To achieve this, we propose the following training and inference methods:

- Stage 1 training: We first train a motion VAE enhanced by adversarial training to achieve high reconstruction/generation performance. We further propose replacing the decoder for adversarial training with a SAN-based one to boost our model performance (Section 3.2).
- Stage 2 training: To reduce computational complexity while simultaneously enabling high-quality text-driven motion generation, we train a text-conditioned diffusion model on the low-dimensional latent space learned by stage 1, i.e., a latent diffusion model (Section 3.3).
- Guided generation: Adopting training-free guided generation in inference enables multiple editing functions required in motion generation without additional training (Section 3.4).

The outline of our text-to-motion generation model, MoLA, is shown in Figure 2.

3.2 Stage 1: Continuous Motion Latent Representation with Adversarial Training

3.2.1 *Learning a rich motion latent representation with VAE-GAN.* We propose a motion variational autoencoder (VAE), enhanced by adversarial training, to learn a low-dimensional latent representation for diverse human motion sequences. Assume an observed motion $\mathbf{x} \in \mathbb{R}^{N \times L}$, where N and L denote raw motion data dimension per frame and motion length, respectively. To learn such a latent representation, we first define a d_z -dimensional latent variable $\mathbf{z} \in \mathbb{R}^{d_z}$, which is assumed to generate data sample \mathbf{x} . The generative process is modeled as $\mathbf{x} \sim p_{\psi}(\mathbf{x}|\mathbf{z})$ with a prior $p(\mathbf{z})$. The prior is assumed to be a standard Gaussian distribution, i.e., $p(\mathbf{z}) = \mathcal{N}(\mathbf{0}, \mathbf{I})$. We model the conditional distribution as a Gaussian distribution: $p_{\psi}(\mathbf{x}|\mathbf{z}) = \mathcal{N}(g_{\psi}(\mathbf{z}), \sigma^2 \mathbf{I})$ with $g_{\psi} : \mathbb{R}^{d_z} \rightarrow \mathbb{R}^{N \times L}$ and $\sigma^2 \in \mathbb{R}_+$, where \mathbb{R}_+ indicates the set of all positive real numbers. As in a usual VAE, we introduce an approximated posterior, which is modeled by a Gaussian distribution as $q_{\eta}(\mathbf{z}|\mathbf{x}) = \mathcal{N}(\boldsymbol{\mu}_{\eta}(\mathbf{x}), \text{diag}(\boldsymbol{\sigma}_{\eta}(\mathbf{x})))$, with $\boldsymbol{\mu}_{\eta} : \mathbb{R}^{N \times L} \rightarrow \mathbb{R}^{d_z}$ and $\boldsymbol{\sigma}_{\eta} : \mathbb{R}^{N \times L} \rightarrow \mathbb{R}_+^{d_z}$. As a result, the VAE consists of an encoder and a decoder, parameterized by η and ψ , respectively. We construct the autoencoder based on a transformer-based architecture [5, 32]. The objective function for the VAE is

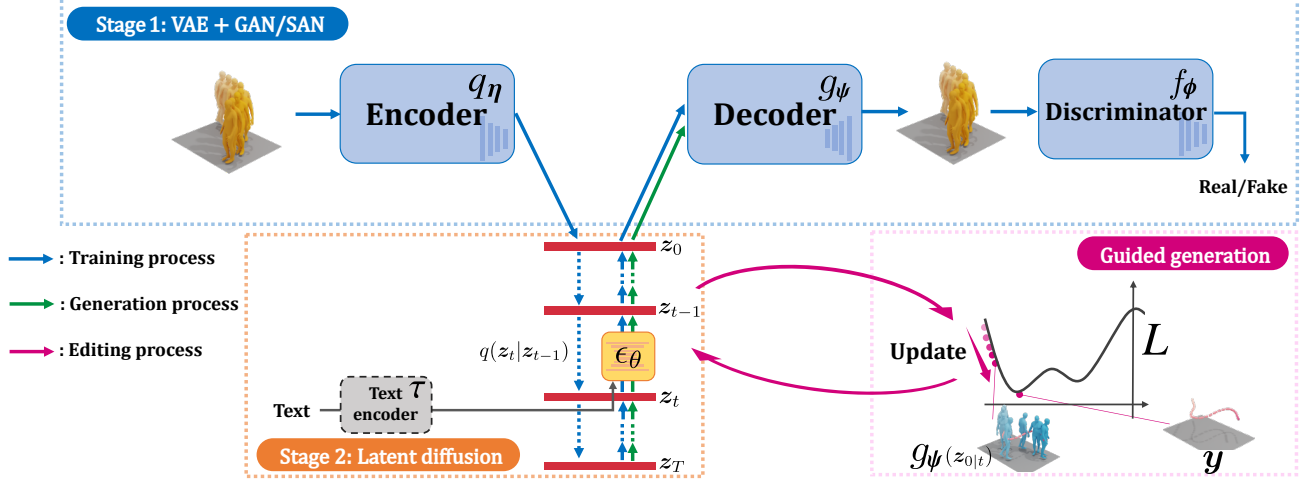


Figure 2: Overall architecture of MoLA. Stage 1: A motion VAE enhanced by adversarial training learns a low-dimensional latent representation for diverse human motion sequences. Stage 2: A text-conditioned latent diffusion model reduces computational costs and enables high-quality text-to-motion generation by utilizing the latent representation obtained in stage 1. Guided generation: During the inference of the stage 2 model, a training-free guided generation method minimizes a loss function L , which can be flexibly set depending on the task, and multiple motion editing tasks can also be performed in a single framework.

formulated as the negative evidence lower bound (negative ELBO) per sample x , which is a summation of mean squared error and KL regularization terms:

$$\mathcal{J}_{\text{VAE}}(\psi, \eta; x) = \mathbb{E}_{q_\eta(z|x)} [\|x - g_\psi(z)\|_2^2] + \lambda_{\text{reg}} D_{\text{KL}}(q_\eta(z|x) \| p(z)), \quad (1)$$

where λ_{reg} is a reciprocal of σ^2 (treated as a hyperparameter in this work). The encoder q_η can be trained to produce a low-dimensional latent representation, and the decoder g_ψ can also be trained to accurately reconstruct the input motion sequences from the latent representations.

To achieve high-quality generation, we need to push the limits of compression. Hence, we propose incorporating adversarial training into the motion VAE. More specifically, we introduce a discriminator, denoted as $f_\phi : \mathbb{R}^{N \times L} \rightarrow \mathbb{R}$, that aims to distinguish real and reconstructed motions. The adversarial training is formulated as a two-player optimization between the VAE and the discriminator. The discriminator is trained by the maximization of $\mathbb{E}_{p(x)} \mathcal{L}_{\text{GAN}}(\phi; \psi, \eta, x)$ with respect to ϕ , where

$$\begin{aligned} \mathcal{L}_{\text{GAN}}(\phi; \psi, \eta, x) = & \min \{0, -1 + f_\phi(x)\} \\ & + \mathbb{E}_{q_\eta(z|x)} [\min \{0, -1 - f_\phi(g_\psi(z))\}]. \end{aligned} \quad (2)$$

We formulate the overall loss for the VAE as a combined objective of the negative ELBO and adversarial loss, as

$$\min_{\phi, \psi} \mathbb{E}_{p(x)} [\mathcal{J}_{\text{VAE}}(\psi, \eta; x) + \lambda_{\text{adv}} \mathcal{L}_{\text{GAN}}(\psi, \eta; \phi, x)], \quad (3)$$

where λ_{adv} is a positive scalar that adjusts the balance between the two terms, and

$$\mathcal{J}_{\text{GAN}}(\psi, \eta; \phi, x) = -\mathbb{E}_{q_\eta(z|x)} [f_\phi(g_\psi(z))]. \quad (4)$$

We train both the VAE and the discriminator with Equations (2) and (3) in an alternating way.

3.2.2 From GAN- to SAN-based discriminator. We apply the SAN framework [47] to further enhance the motion VAE based on a prior report showing that a model with a SAN-based discriminator has achieved SOTA performance in image generation. Takida *et al.* [47] incorporated a sliced optimal transport perspective into a general GAN. Following this work, we first decompose the discriminator f_ϕ into the last linear layer and the remaining neural part, denoted as $w \in \mathbb{R}^{d_w}$ and $h_\phi : \mathbb{R}^{N \times L} \rightarrow \mathbb{R}^{d_w}$ with $d_w \in \mathbb{N}$, respectively. This decomposition provides an interpretation of the discriminator: the neural function h_ϕ maps motion sequences to non-linear features, and then the linear layer w projects them into scalars. As a preliminary step for applying SAN to the adversarial training in Section 3.2.1, we normalize w using its norm, resulting in $\omega = w / \|w\|_2$, which indicates the direction of the projecting. Now, the discriminator is represented in the form of an inner product as $f_\phi(x) = \omega^\top h_\phi(x)$, and its parameter is $\phi = \{\phi, \omega\}$.

The prior work has shown that the discriminator obtained from the optimal solution of ω in the hinge loss (2) does not guarantee gradients that make the generated distribution close to the data distribution. To address this issue, we adopt the SAN maximization problem instead of Equation (2). Specifically, we optimize the neural part ϕ with the original hinge loss, while applying the Wasserstein GAN loss [2] to the direction ω . The modified maximization objective is formulated as

$$\begin{aligned} \mathcal{L}_{\text{SAN}}(\phi; \psi, \eta, x) = & \mathcal{L}_{\text{GAN}}(\{\phi, \omega^-\}; \psi, \eta, x) \\ & + \omega^\top (h_{\phi^-}(x) - \mathbb{E}_{q_\eta(z|x)} [h_{\phi^-}(g_\psi(z))]), \end{aligned} \quad (5)$$

where $(\cdot)^-$ indicates a stop gradient operator. The second term in Equation (5) induces the direction that best discriminates between the real and generated sample sets in the feature space. We employ the same minimization objective as defined in Equation (3).

3.3 Stage 2: Motion Latent Diffusion

In this section, we train a text-conditioned diffusion model on the low-dimensional motion latent space obtained by the autoencoder learned in the stage 1 (Section 3.2). Using the trained model, we perform motion generation conditioned on text. First, we define a time-dependent sequence $z = z_0, z_1, \dots, z_t, \dots, z_T \in \mathbb{R}^{d_z}$ starting from the VAE encoder output $z \sim q_\eta(z|x)$, which is derived from the following Markov diffusion process in the latent space:

$$q(z_t|z_{t-1}) = \mathcal{N}(\sqrt{\alpha_t}z_{t-1}, (1-\alpha_t)\mathbf{I}), \quad (6)$$

where $T > 0$ and the constant $\alpha_t \in (0, 1)$ is a pre-defined noise-scheduling parameter that determines the forward process. The forward process allows for the sampling of z_t at an arbitrary time step t in a closed form: $z_t = \sqrt{\alpha_t}z_0 + \sqrt{1-\alpha_t}\epsilon$, where $\bar{\alpha}_t := \prod_{s=1}^t \alpha_s$ and $\epsilon \sim \mathcal{N}(\mathbf{0}, \mathbf{I})$.

The diffusion model is trained to reverse the diffusion process described in Equation (6), i.e., to perform denoising. Specifically, the model learns to estimate the noise component ϵ in the noisy sample z_t as in the following objective:

$$\mathcal{J}_{\text{LDM}}(\theta) = \mathbb{E}_{z_0, \epsilon, t} [\|\epsilon - \epsilon_\theta(z_t, t)\|_2^2], \quad (7)$$

where θ is the model parameter to be trained, and the time step t is uniformly sampled from $\{1, \dots, T\}$.

As our goal is text-to-motion generation, our interest is in the conditional distribution $p(z|c)$ conditioned on the text prompt c . Here, similar to many text-conditioned latent diffusion models [5, 39], we train the conditional model $\epsilon_\theta(z_t, t, \tau(c))$ conditioned on the output of a text encoder $\tau(c)$, using the following objective function:

$$\mathcal{J}_{\text{LDM}}(\theta) = \mathbb{E}_{\{z_0, c\}, \epsilon, t} [\|\epsilon - \epsilon_\theta(z_t, t, \tau(c))\|_2^2], \quad (8)$$

where z_0 and c are drawn from the joint empirical distribution. In addition, following many other works, we adopt classifier-free guidance [17] and train the model unconditionally i.e., without a text prompt, with a certain probability during training.

During the inference (text-to-motion generation), the trained diffusion model $\epsilon_\theta(z_t, t, \tau(c))$ is employed to generate z_0 through a denoising process conditioned on the text prompt c . We adopt the sampling scheme of DDIM [43], in which each sampling step is defined as:

$$\begin{aligned} z_{t-1} &= \sqrt{\bar{\alpha}_{t-1}} \left(\frac{z_t - \sqrt{1-\bar{\alpha}_{t-1}}\epsilon_\theta(z_t, t, \tau(c))}{\sqrt{\alpha_t}} \right) \\ &+ \sqrt{1-\bar{\alpha}_{t-1} - \sigma_t^2} \epsilon_\theta(z_t, t, \tau(c)) + \sigma_t \epsilon, \end{aligned} \quad (9)$$

where $\sigma_t > 0$ determines the stochasticity of the sampling process, and the sampling process becomes deterministic when $\sigma_t = 0$. The part $(z_t - \sqrt{1-\bar{\alpha}_{t-1}}\epsilon_\theta(z_t, t, \tau(c)))/\sqrt{\alpha_t}$ in the first term corresponds to a direct estimate of the clean latent z_0 from the noisy sample z_t using the diffusion model based on Tweedie's formula [8]; this estimate is denoted as $z_{0|t}$.

3.4 Controllable Motion Generation on Latent Diffusion Sampling

In this section, we present a guided generation framework that leverages the pre-trained motion latent diffusion model (Section 3.3) for

conditional motion generation and editing tasks without extra training. Major training-free methods such as DPS [6], FreeDoM [54], and MPGD [16] are based on the fact that the conditional score function can be decomposed into two additive terms: the unconditional score function and the log-likelihood term. Specifically, for a new condition y , we have

$$\nabla_{z_t} \log p(z_t|c, y) = \nabla_{z_t} \log p(z_t|c) + \nabla_{z_t} \log p(y|z_t, c), \quad (10)$$

as derived from Bayes' rule. The conditional generation based on the aforementioned property can be regarded as a sequential procedure implemented as follows. First, from z_t , a denoised sample z_{t-1} is obtained by the sampling step in Equation (9), without considering the given condition y . Subsequently, z_{t-1} is further updated using the gradient with respect to z_t for the log-likelihood term.

The log-likelihood term is defined for noisy sample z_t . In the classifier-guided diffusion [46], time-dependent classifiers for z_t have to be trained, which requires additional training. In contrast, in training-free methods such as DPS, FreeDoM, and MPGD, this term is approximated with the current clean data estimate $z_{0|t}$ and a loss function $L(x; y)$ defined for clean data. This loss function can be flexibly set depending on the task. For example, in inverse problems of the form $y = \mathcal{A}(x)$, where \mathcal{A} is a differentiable function with respect to x , the loss function can be set as $\|y - \mathcal{A}(x_{0|t})\|_2^2$, where $x_{0|t} = g_\psi(z_{0|t})$ is a clean data estimate in the original data domain and obtained through the VAE decoder. In FreeDoM's FaceID-guided generation, the ℓ_2 distance of features obtained by inputting facial images into a facial recognition model is used as the loss.

Here, we adopt MPGD [16], a fast yet high-quality guidance method applicable to latent diffusion models. Following the denoising step, it updates the denoised sample for the loss function $L(x; y)$ as follows:

$$z_{t-1} \leftarrow z_{t-1} - \rho_t \sqrt{\bar{\alpha}_{t-1}} \nabla_{z_{0|t}} L(g_\psi(z_{0|t}); y), \quad (11)$$

where ρ_t is a time-dependent step size parameter.

More specifically, in editing motion tasks we generate motions to match given specific poses or a trajectory control signal. To deal with various motion editing tasks in this framework, the loss functions are designed as follows:

$$L(g_\psi(z_{0|t}); y) = \sum_n \sum_l m_{nl} \|R(g_\psi(z_{0|t}))_{nl} - y_{nl}\|_2, \quad (12)$$

where n and l are indices of joint and frame, respectively, and m_{nl} is a binary value indicating whether the control position y_{nl} contains a valid value at frame l for joint n , and $R(\cdot)$ is a function to convert the motion features including the joint's local positions to global absolute locations. We set L for the guided generation to measure the distance between desired constraints y and the joint locations of the generated motion. Target locations as constraint y can be specified for any subset of joints in any subset of motion frames.¹ Editing a generated motion to match specific poses or to follow a

¹As examples of motion editing, if y is given as the start-end positions, we can handle the motion in-betweening. If y is given as the lower body positions, we can edit the upper body corresponding to the lower one. If y is given as the pelvis trajectory, it corresponds to the path-following task. We leave the task details to Section 4.5. Note that the guided generation framework in Equations (11) and (12) has the potential to generate motion while dealing with a variety of time and spatial constraints not limited to these three task examples.

| Dataset | Stage 1 model | rFID \downarrow |
|-----------|---------------|-------------------|
| HumanML3D | VAE | 0.206 |
| | VAE + GAN | 0.179 |
| | VAE + SAN | 0.141 |
| KIT-ML | VAE | 0.311 |
| | VAE + GAN | 0.293 |
| | VAE + SAN | 0.280 |

Table 2: Analysis of motion reconstruction performance (training stage 1 with VAE) on HumanML3D and KIT-ML

| Dataset | Stage 1 model | rFID \downarrow |
|-----------|---------------|-------------------|
| HumanML3D | VQ-VAE | 0.065 |
| | VQ-VAE + GAN | 0.057 |
| | VQ-VAE + SAN | 0.051 |
| KIT-ML | VQ-VAE | 0.665 |
| | VQ-VAE + GAN | 0.377 |
| | VQ-VAE + SAN | 0.299 |

Table 3: Analysis of motion reconstruction performance (training stage 1 with VQ-VAE) on HumanML3D and KIT-ML

specific trajectory can be achieved by minimizing L with the update rule in Equation (11).

4 EXPERIMENTS

4.1 Datasets

We conduct empirical evaluations on two widely used datasets for text-to-motion generation: HumanML3D [14] and KIT Motion-Language (KIT-ML) [36]. **HumanML3D** contains 14,616 human motions from the AMASS [28] and HumanAct12 [15] datasets and 44,970 text descriptions. **KIT-ML** contains 3,911 human motion sequences from the KIT [29] and CMU [7] datasets and 6,278 textual descriptions. Both datasets are split into training, validation, and test sets with proportions of 80%, 5% and 15%, respectively.

4.2 Implementation Details

In our experiment, we train two different types of models, as follows. (i) We train the motion VAE and discriminator f_ϕ described in Section 3.2 and use these stage 1 models to train the stage 2 model ϵ_θ . (ii) We train the motion VQ-VAE in T2M-GPT [56] and the discriminator, and train the transformer model in the latter stage to generate code indices conditioned on the text description. Case (ii) is intended to verify whether adversarial training is also effective in a VQ-based text-to-motion framework.

In case (i), the motion VAE architecture is based on the VAE part in MLD [5]. The encoder q_θ and decoder g_ϕ of the VAE model all consist of nine layers and four heads with skip connection. For adversarial training, we use the discriminator f_ϕ whose architecture is composed of 1D convolution, residual block, and Leaky ReLU. We set $\lambda_{\text{adv}} = 1.0 \times 10^{-3}$ as the weight for adversarial training. All our models are trained for 6K epochs with the AdamW optimizer using the batch size of 128 and a cosine-annealing learning rate of 1.0×10^{-4} with a warm-up. All other settings, including those for the stage 2 model ϵ_θ training and text embedding $\tau(c)$, follow the official MLD implementation.

In case (ii), we use motion VQ-VAE whose codebook size is set to 512×512 . We utilize the AdamW optimizer, batch size of 256, and exponential moving constant of 0.99. For adversarial training, we use the discriminator f_ϕ whose architecture is composed of 1D convolution, residual block, and Leaky ReLU, the same as in case (i). We train the first 200K iterations with a learning rate of 2.0×10^{-4} , and 100K with a learning rate of 1.0×10^{-5} . All other settings follow the official T2M-GPT implementation.

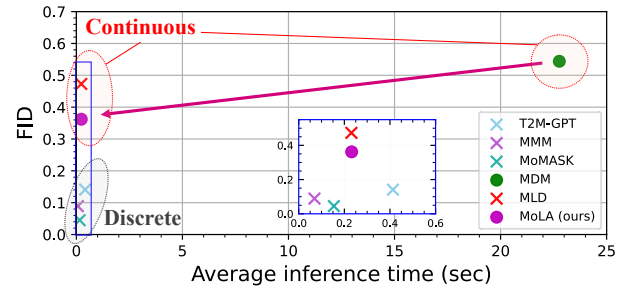


Figure 3: Comparison of inference cost, generation performance, and editability for text-to-motion methods. ● means a method that can edit motion in a training-free manner, and ✕ means a method that cannot edit motion in a training-free manner. We calculate the average inference time on the test set of HumanML3D without model or data loading parts. All tests are performed on the same NVIDIA A100 GPU.

4.3 Effectiveness of Adversarial Training

We first discuss the effect of adversarial training on Stage 1. Here, we adopt VAE and VQ-VAE described in Section 4.2 as the baselines. The case of VAE is intended to show the effects in a continuous latent space, while the case of VQ-VAE is intended to show the effects in a discrete latent space. The results for VAE combined with GAN/SAN are shown in Table 2, and those of VQ-VAE in Table 3. We utilize the reconstruction FID (rFID) as an evaluation metric. As shown in the tables, the adversarial training is effective in both VAE and VQ-VAE in the motion reconstruction task. In particular, we can improve the performance of the Stage 1 model by adopting the SAN framework instead of the conventional GAN. A better rFID is directly related to the upper bound of the overall performance of a text-to-motion model. Thus, we use VAE trained with the SAN framework for our MoLA. We demonstrate that adversarial training in Stage 1 actually improves the generation performance of the entire model in the next section.

4.4 Motion Generation

Next, we evaluate inference cost and quality of generation in comparison to existing text-to-motion methods that have publicly available implementations [5, 13, 35, 49, 56]. Since our requirements are

| Category | Method | R-Precision \uparrow | | | FID \downarrow | MMDist \downarrow | Diversity \rightarrow | MModality \uparrow |
|-----------------------|--------------------|------------------------|------------------|------------------|------------------|---------------------|-------------------------|----------------------|
| | | Top-1 | Top-2 | Top-3 | | | | |
| N/A | Real motion data | 0.511 \pm .003 | 0.703 \pm .003 | 0.797 \pm .002 | 0.002 \pm .000 | 2.974 \pm .008 | 9.503 \pm .065 | - |
| Discrete | M2DM [23] | 0.497 \pm .003 | 0.682 \pm .002 | 0.763 \pm .003 | 0.352 \pm .005 | 3.134 \pm .010 | 9.926 \pm .073 | 3.587 \pm .072 |
| | AttT2M [59] | 0.499 \pm .003 | 0.690 \pm .002 | 0.786 \pm .002 | 0.112 \pm .006 | 3.038 \pm .007 | 9.700 \pm .090 | 2.452 \pm .051 |
| | T2M-GPT [56] | 0.492 \pm .003 | 0.679 \pm .002 | 0.775 \pm .002 | 0.141 \pm .005 | 3.121 \pm .009 | 9.722 \pm .081 | 1.831 \pm .048 |
| | MoMask [13] | 0.521 \pm .002 | 0.713 \pm .002 | 0.807 \pm .002 | 0.045 \pm .002 | 2.958 \pm .008 | - | 1.241 \pm .040 |
| | DiverseMotion [26] | 0.496 \pm .004 | 0.687 \pm .004 | 0.783 \pm .003 | 0.070 \pm .004 | 3.063 \pm .011 | 9.551 \pm .068 | 2.062 \pm .079 |
| | MMM [35] | 0.504 \pm .003 | 0.696 \pm .003 | 0.794 \pm .002 | 0.080 \pm .003 | 2.998 \pm .007 | 9.411 \pm .058 | 1.164 \pm .041 |
| Continuous (raw data) | MotionDiffuse [58] | 0.491 \pm .001 | 0.681 \pm .001 | 0.782 \pm .001 | 0.630 \pm .001 | 3.113 \pm .001 | 9.410 \pm .049 | 1.553 \pm .042 |
| | MDM [49] | 0.320 \pm .005 | 0.498 \pm .004 | 0.611 \pm .007 | 0.544 \pm .044 | 5.566 \pm .027 | 9.559 \pm .086 | 2.799 \pm .072 |
| | Fg-T2M [51] | 0.492 \pm .002 | 0.683 \pm .003 | 0.783 \pm .002 | 0.243 \pm .019 | 3.109 \pm .007 | 9.278 \pm .072 | 1.614 \pm .049 |
| Continuous (latent) | MLD [5] | 0.481 \pm .003 | 0.673 \pm .003 | 0.772 \pm .002 | 0.473 \pm .013 | 3.196 \pm .010 | 9.724 \pm .082 | 2.413 \pm .079 |
| | MoLA (ours) | 0.514 \pm .003 | 0.705 \pm .002 | 0.797 \pm .002 | 0.362 \pm .009 | 3.162 \pm .008 | 9.672 \pm .079 | 2.355 \pm .121 |

Table 4: Comparison with state-of-the-art methods on HumanML3D.

1) fast generation, 2) high generation performance, and 3) training-free editing, we apply adversarial training to a continuous latent case, specifically MLD [5] (introduced in Section 3) We show that our proposed strategy improves MLD and achieves a better performance in Figure 3. Note that the difference between the MLD baseline and our MoLA is the training method, not the inference. Thus, as shown in Figure 3, inference with our model can be achieved with equivalent time to the MLD baseline, which is much faster in generation than data-space diffusion MDM [49] that is the only existing method that can perform training-free motion editing. It is true that most methods based on discrete representation perform very well in terms of fidelity and speed, but there is no discrete method that can deal with multiple editing tasks in a training-free manner and satisfies our requirements.

In addition, we evaluate our proposed MoLA in comparison to current SOTA methods [5, 13, 26, 35, 49, 51, 56, 58, 59] using five metrics (R-Precision, Fréchet Inception Distance (FID), Multimodal distance (MMDist), Diversity, and MultiModality (MModality)) proposed by Guo *et al.* [14]. For evaluation, we select the model that achieves the best FID, which is a metric that evaluates the overall motion quality, on the validation set and report its performance on the test set on each of the two datasets. We show the results in Tables 4 and 5. The methods are organized into three groups: i) those using VQ-based latent representations (**Discrete**), ii) those using data-space diffusion model (**Continuous (raw data)**), and iii) those using VAE-based latent representations (**Continuous (latent)**). The discrete approaches perform well in motion generation (e.g., [13, 26, 35]). However, those models cannot control an arbitrary set of joints in a training-free manner [35] as we have discussed so far. MDM [49], MotionDiffuse [58] and Fg-T2M [51] adopt data-space diffusion, while MLD [5] and our MoLA utilize a diffusion model in a low-dimensional latent space. Therefore, the former are grouped in Continuous (raw data) and the latter in Continuous (latent) in the tables. As shown in Figure 3, MLD and our MoLA can be much faster in generation than MDM, which is the only existing method that can perform training-free motion editing. Moreover, MoLA achieves a better performance than MLD, especially in the R-precision, FID, and MMDist metrics on both HumanML3D and KIT-ML datasets as shown in the tables. As we will show in the next section, our MoLA can also deal with multiple

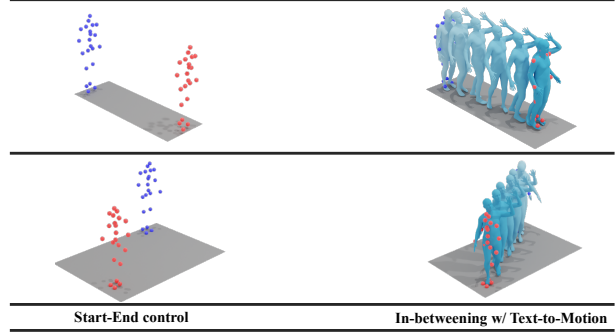


Figure 4: Qualitative results of motion in-betweening task. Blue and red points are used as inputs to constrain the start and end positions, respectively. These are the results generated by our framework from the same text prompt (“A person walks while raising his left hand.”) for two different start-end positions.

motion editing tasks without additional training, which means our MoLA satisfies our three requirements best.

4.5 Motion Editing

Here, we demonstrate three different types of editing tasks with a single framework: editing in the time direction (in-betweening), editing in some joints of motion (upper body editing), and editing with the path specified as the trajectory (path following). We experiment with the following motion editing on models trained in HumanML3D [14].

In-betweening: Motion in-betweening is an important editing task that interpolates or fills the gaps between keyframes or major motion joints to create smooth 3D motion animation. In our framework, by applying the update rule of MPGD [16] on latent space (Section 3.4), it is easy to coordinate and generate motion between past and future contexts without additional training. We only need to set the start-end positions or the motions of a few frames as the control signal \mathbf{y} in (12). The motion in-betweening results with our model when different start-end controls are given as \mathbf{y} in the same text condition are shown in Figure 4.

| Category | Method | R-Precision \uparrow | | | FID \downarrow | MMDist \downarrow | Diversity \rightarrow | MModality \uparrow |
|-----------------------|--------------------|------------------------|------------------|------------------|------------------|---------------------|-------------------------|----------------------|
| | | Top-1 | Top-2 | Top-3 | | | | |
| N/A | Real motion data | 0.424 \pm .005 | 0.649 \pm .006 | 0.779 \pm .006 | 0.031 \pm .004 | 2.788 \pm .012 | 11.08 \pm .097 | - |
| Discrete | M2DM [23] | 0.416 \pm .004 | 0.628 \pm .004 | 0.743 \pm .004 | 0.515 \pm .029 | 3.015 \pm .017 | 11.417 \pm .97 | 3.325 \pm .37 |
| | AttT2M [59] | 0.413 \pm .006 | 0.632 \pm .006 | 0.751 \pm .006 | 0.870 \pm .039 | 3.039 \pm .021 | 10.96 \pm .123 | 2.281 \pm .047 |
| | T2M-GPT [56] | 0.416 \pm .006 | 0.627 \pm .006 | 0.745 \pm .006 | 0.514 \pm .029 | 3.007 \pm .029 | 10.921 \pm .108 | 1.570 \pm .039 |
| | MoMask [13] | 0.433 \pm .007 | 0.656 \pm .005 | 0.781 \pm .005 | 0.204 \pm .011 | 2.779 \pm .022 | - | 1.131 \pm .043 |
| | DiverseMotion [26] | 0.416 \pm .005 | 0.637 \pm .008 | 0.760 \pm .011 | 0.468 \pm .098 | 2.892 \pm .041 | 10.873 \pm .101 | 2.062 \pm .079 |
| | MMM [35] | 0.381 \pm .005 | 0.590 \pm .006 | 0.718 \pm .005 | 0.429 \pm .019 | 3.146 \pm .019 | 10.633 \pm .097 | 1.105 \pm .026 |
| Continuous (raw data) | MotionDiffuse [58] | 0.417 \pm .004 | 0.621 \pm .004 | 0.739 \pm .004 | 1.954 \pm .062 | 2.958 \pm .005 | 11.10 \pm .143 | 0.730 \pm .013 |
| | MDM [49] | 0.164 \pm .004 | 0.291 \pm .004 | 0.396 \pm .004 | 0.497 \pm .021 | 9.191 \pm .022 | 10.847 \pm .109 | 1.907 \pm .214 |
| | Fg-T2M [51] | 0.418 \pm .005 | 0.626 \pm .004 | 0.745 \pm .004 | 0.571 \pm .047 | 3.114 \pm .015 | 10.93 \pm .083 | 1.019 \pm .029 |
| Continuous (latent) | MLD [5] | 0.390 \pm .008 | 0.609 \pm .008 | 0.734 \pm .007 | 0.404 \pm .027 | 3.204 \pm .027 | 10.80 \pm .117 | 2.192 \pm .071 |
| | MoLA (ours) | 0.401 \pm .004 | 0.612 \pm .004 | 0.728 \pm .004 | 0.350 \pm .020 | 3.187 \pm .027 | 10.88 \pm .110 | 2.226 \pm .097 |

Table 5: Comparison with state-of-the-art methods on KIT-ML.

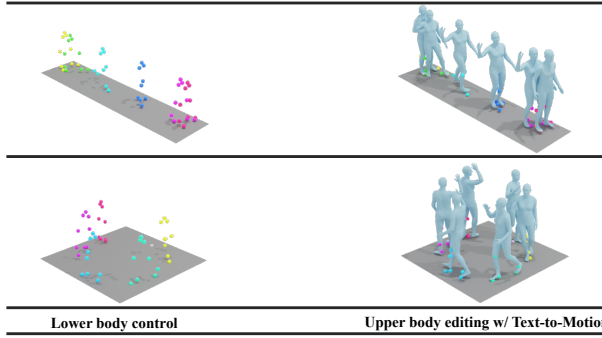


Figure 5: Qualitative results of upper body editing task. Each colored point is used inputs to control the lower body position as a constraint. These are the results generated by our framework from the same text prompt (“A person puts his right hand to the air.”) for two different lower body positions.

Upper body editing: Upper body editing combines generated upper body parts with given lower body parts. Generating certain joints to fit given body parts can be seen as the task of outpainting in the spatial dimension of motion. In our framework, similar to the motion in-betweening, the loss and its gradient are calculated in the data-space as (11), and sampling is performed taking into account its gradients. The control signal \mathbf{y} in (12) is set as lower body positions that is not subject to editing. Note that although we are dealing with upper body editing in these experiments, it is in principle possible to specify a different joint subset. Therefore, without the need for a separate architecture or additional training, our framework allows editing conditioned on given body parts of motion. The upper body editing results with our model when different lower body controls are given as \mathbf{y} in the same text condition are shown in Figure 5.

Path-following: Path-following motion generation is a task of giving a trajectory (often the position of the pelvis) and generating the motion that matches with the given route. Controlling the trajectory of generated motion can lead to more motion variation, avoidance of obstacles, and the creation of motion that meets physical constraints. Our framework can edit a motion to follow a

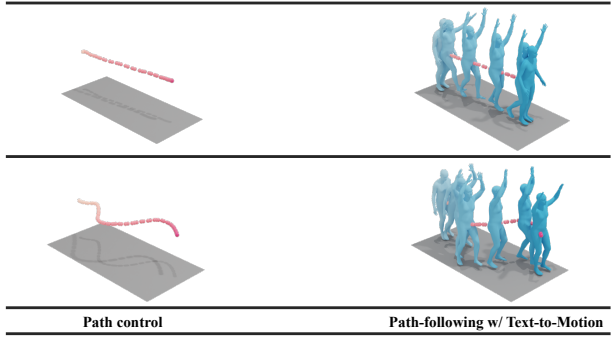


Figure 6: Qualitative results of path-following task. The points are the input to control a motion trajectory. These are the results generated by our framework from the same text prompt (“A person walks with his hands up.”) for two different given trajectories.

specific path by minimizing the loss between a joint of the generated motion and a desired trajectory of the joint, similar to motion in-betweening. In this experimental case, the desired pelvis trajectory is set as the control signal \mathbf{y} in (12). The path-following generation results with our model when different path controls are given as \mathbf{y} in the same text condition are shown in Figure 6.

5 CONCLUSION

In this paper, we proposed MoLA, a text-to-motion model that achieves fast, high-quality generation with multiple control tasks in a single framework. To construct our model, we employed a latent diffusion-based method, and introduced adversarial training. In addition, we applied a training-free guided generation framework based on MPG. The results of quantitative evaluation demonstrate the effectiveness of adversarial training in the text-to-motion generation. In particular, we found that replacing GAN with SAN boosts the performance of our model. We also showed that our model can perform motion in-betweening, upper body editing, and path following within a single framework.

REFERENCES

[1] Chaitanya Ahuja and Louis-Philippe Morency. 2019. Language2Pose: Natural Language Grounded Pose Forecasting. In *Proc. International Conference on 3D Vision (3DV)*.

[2] Martin Arjovsky, Soumith Chintala, and Léon Bottou. 2017. Wasserstein Generative Adversarial Networks. In *Proc. International Conference on Machine Learning (ICML)*.

[3] Huiwen Chang, Han Zhang, Jarred Barber, Aaron Maschinot, Jose Lezama, Lu Jiang, Ming-Hsuan Yang, Kevin Patrick Murphy, William T. Freeman, Michael Rubinstein, Yuanzhen Li, and Dilip Krishnan. 2023. Muse: Text-To-Image Generation via Masked Generative Transformers. In *Proc. International Conference on Machine Learning (ICML)*.

[4] Huiwen Chang, Han Zhang, Lu Jiang, Ce Liu, and William T Freeman. 2022. Maskgit: Masked generative image transformer. In *Proc. IEEE/CVF Conference on Computer Vision and Pattern Recognition (CVPR)*.

[5] Xin Chen, Biao Jiang, Wen Liu, Zilong Huang, Bin Fu, Tao Chen, and Gang Yu. 2023. Executing your Commands via Motion Diffusion in Latent Space. In *Proc. IEEE/CVF Conference on Computer Vision and Pattern Recognition (CVPR)*.

[6] Hyungjin Chung, Jeongsol Kim, Michael Thompson Mccann, Marc Louis Klasky, and Jong Chul Ye. 2023. Diffusion Posterior Sampling for General Noisy Inverse Problems. In *Proc. International Conference on Learning Representation (ICLR)*.

[7] CMU 2003. CMU Graphics Lab Motion Capture Database. <http://mocap.cs.cmu.edu/>. (Accessed: 2024-02-08.).

[8] Bradley Efron. 2011. Tweedie's formula and selection bias. *J. Amer. Statist. Assoc.* 106, 496 (2011), 1602–1614.

[9] Patrick Esser, Robin Rombach, and Bjorn Ommer. 2021. Taming transformers for high-resolution image synthesis. In *Proc. IEEE/CVF Conference on Computer Vision and Pattern Recognition (CVPR)*.

[10] Shanghua Gao, Pan Zhou, Ming-Ming Cheng, and Shuicheng Yan. 2023. Masked diffusion transformer is a strong image synthesizer. In *Proc. IEEE/CVF Conference on Computer Vision and Pattern Recognition (CVPR)*.

[11] Ian Goodfellow, Jean Pouget-Abadie, Mehdi Mirza, Bing Xu, David Warde-Farley, Sherjil Ozair, Aaron Courville, and Yoshua Bengio. 2014. Generative adversarial nets. In *Proc. Advances in Neural Information Processing Systems (NeurIPS)*.

[12] Shuyang Gu, Dong Chen, Jianmin Bao, Fang Wen, Bo Zhang, Dongdong Chen, Lu Yuan, and Baining Guo. 2022. Vector Quantized Diffusion Model for Text-to-Image Synthesis. In *Proc. IEEE/CVF Conference on Computer Vision and Pattern Recognition (CVPR)*.

[13] Chuan Guo, Yuxuan Mu, Muhammad Gohar Javed, Sen Wang, and Li Cheng. 2023. MoMask: Generative Masked Modeling of 3D Human Motions. In *Proc. IEEE/CVF Conference on Computer Vision and Pattern Recognition (CVPR)*.

[14] Chuan Guo, Shihao Zou, Xinxin Zuo, Sen Wang, Wei Ji, Xingyu Li, and Li Cheng. 2022. Generating diverse and natural 3d human motions from text. In *Proc. IEEE/CVF Conference on Computer Vision and Pattern Recognition (CVPR)*.

[15] Chuan Guo, Xinxin Zuo, Sen Wang, Shihao Zou, Qingyao Sun, Annan Deng, Minglun Gong, and Li Cheng. 2020. Action2motion: Conditioned generation of 3d human motions. In *Proc. ACM International Conference on Multimedia (ACM MM)*.

[16] Yutong He, Naoki Murata, Chieh-Hsin Lai, Yuhta Takida, Toshimitsu Uesaka, Dongjun Kim, Wei-Hsiang Liao, Yuki Mitsuishi, J Zico Kolter, Ruslan Salakhutdinov, and Stefano Ermon. 2024. Manifold Preserving Guided Diffusion. In *Proc. International Conference on Learning Representation (ICLR)*.

[17] Jonathan Ho and Tim Salimans. 2022. Classifier-free diffusion guidance. *arXiv preprint arXiv:2207.12598* (2022).

[18] Vladimir Lashin and Esa Rahtu. 2021. Taming Visually Guided Sound Generation. In *Proc. British Machine Vision Conference (BMVC)*.

[19] Biao Jiang, Xin Chen, Wen Liu, Jingyi Yu, Gang Yu, and Tao Chen. 2023. MotionGPT: Human Motion as a Foreign Language. In *Proc. Advances in Neural Information Processing Systems (NeurIPS)*.

[20] Korrawe Karunratanakul, Konpat Preechakul, Emre Aksan, Thabo Beeler, Supasorn Suwajanakorn, and Siyu Tang. 2023. Optimizing Diffusion Noise Can Serve As Universal Motion Priors. *arXiv preprint arXiv:2312.11994* (2023).

[21] Korrawe Karunratanakul, Konpat Preechakul, Supasorn Suwajanakorn, and Siyu Tang. 2023. Guided motion diffusion for controllable human motion synthesis. In *Proc. IEEE/CVF International Conference on Computer Vision (ICCV)*.

[22] Diederik P Kingma and Max Welling. 2013. Auto-encoding variational bayes. In *Proc. International Conference on Learning Representation (ICLR)*.

[23] Hanyang Kong, Kehong Gong, Dongze Lian, Michael Bi Mi, and Xincho Wang. 2023. Priority-Centric Human Motion Generation in Discrete Latent Space. In *Proc. IEEE/CVF Conference on Computer Vision and Pattern Recognition (CVPR)*.

[24] Doyup Lee, Chiheon Kim, Saehoon Kim, Minsu Cho, and Wook-Shin Han. 2022. Autoregressive Image Generation using Residual Quantization. In *Proc. IEEE/CVF Conference on Computer Vision and Pattern Recognition (CVPR)*.

[25] Haohu Liu, Zehua Chen, Yi Yuan, Xinhao Mei, Xubo Liu, Danilo Mandic, Wenwu Wang, and Mark D Plumley. 2023. AudioLDM: Text-to-Audio Generation with Latent Diffusion Models. In *Proc. International Conference on Machine Learning (ICML)*.

[26] Yunhong Lou, Linchao Zhu, Yaxiong Wang, Xiaohan Wang, and Yi Yang. 2023. Diversemotion: Towards diverse human motion generation via discrete diffusion. *arXiv preprint arXiv:2309.01372* (2023).

[27] Andreas Lugmayr, Martin Daneljan, Andres Romero, Fisher Yu, Radu Timofte, and Luc Van Gool. 2022. RePaint: Inpainting using denoising diffusion probabilistic models. In *Proc. IEEE/CVF Conference on Computer Vision and Pattern Recognition (CVPR)*.

[28] Naureen Mahmood, Nima Ghorbani, Nikolaus F Troje, Gerard Pons-Moll, and Michael J Black. 2019. AMASS: Archive of motion capture as surface shapes. In *Proc. IEEE/CVF Conference on Computer Vision and Pattern Recognition (CVPR)*.

[29] Christian Mandery, Ömer Terlemez, Martin Do, Nikolaus Vahrenkamp, and Tamim Asfour. 2015. The KIT whole-body human motion database. In *Proc. IEEE International Conference on Advanced Robotics (ICAR)*.

[30] Chenlin Meng, Yutong He, Yang Song, Jiaming Song, Jiajun Wu, Jun-Yan Zhu, and Stefano Ermon. 2022. SDEdit: Guided Image Synthesis and Editing with Stochastic Differential Equations. In *Proc. International Conference on Learning Representation (ICLR)*.

[31] William Peebles and Saining Xie. 2023. Scalable diffusion models with transformers. In *Proc. IEEE/CVF Conference on Computer Vision and Pattern Recognition (CVPR)*.

[32] Mathis Petrovich, Michael J Black, and Güл Varol. 2021. Action-conditioned 3d human motion synthesis with transformer vae. In *Proc. IEEE/CVF Conference on Computer Vision and Pattern Recognition (CVPR)*.

[33] Mathis Petrovich, Michael J Black, and Güл Varol. 2022. TEMOS: Generating diverse human motions from textual descriptions. In *Proc. European Conference on Computer Vision (ECCV)*.

[34] Mathis Petrovich, Michael J Black, and Güл Varol. 2023. TMR: Text-to-Motion Retrieval Using Contrastive 3D Human Motion Synthesis. In *Proc. IEEE/CVF Conference on Computer Vision and Pattern Recognition (CVPR)*.

[35] Ekkasit Pinyoanuntapong, Pu Wang, Minwoo Lee, and Chen Chen. 2024. MMM: Generative Masked Motion Model. In *Proc. IEEE/CVF Conference on Computer Vision and Pattern Recognition (CVPR)*.

[36] Matthias Plappert, Christian Mandery, and Tamim Asfour. 2016. The KIT motion-language dataset. *Big data* 4, 4 (2016), 236–252.

[37] Aditya Ramesh, Prafulla Dhariwal, Alex Nichol, Casey Chu, and Mark Chen. 2022. Hierarchical text-conditional image generation with clip latents. *arXiv preprint arXiv:2204.06125* 1, 2 (2022), 3.

[38] Ali Razavi, Aaron van den Oord, and Oriol Vinyals. 2019. Generating diverse high-fidelity images with VQ-VAE-2. In *Proc. Advances in Neural Information Processing Systems (NeurIPS)*.

[39] Robin Rombach, Andreas Blattmann, Dominik Lorenz, Patrick Esser, and Björn Ommer. 2022. High-resolution image synthesis with latent diffusion models. In *Proc. IEEE/CVF Conference on Computer Vision and Pattern Recognition (CVPR)*.

[40] Lita Rout, Negin Raouf, Giannis Daras, Constantine Caramanis, Alex Dimakis, and Sanjay Shakkottai. 2023. Solving Linear Inverse Problems Provably via Posterior Sampling with Latent Diffusion Models. In *Proc. Advances in Neural Information Processing Systems (NeurIPS)*.

[41] Chitwan Saharia, William Chan, Saurabh Saxena, Lala Li, Jay Whang, Emily L Denton, Kamyar Ghasemipour, Raphael Gontijo Lopes, Burcu Karagol Ayan, Tim Salimans, et al. 2022. Photorealistic text-to-image diffusion models with deep language understanding. In *Proc. Advances in Neural Information Processing Systems (NeurIPS)*, Vol. 35.

[42] Jascha Sohl-Dickstein, Eric Weiss, Niru Maheswaranathan, and Surya Ganguli. 2015. Deep unsupervised learning using nonequilibrium thermodynamics. In *Proc. International Conference on Machine Learning (ICML)*.

[43] Jiaming Song, Chenlin Meng, and Stefano Ermon. 2021. Denoising Diffusion Implicit Models. *Proc. International Conference on Learning Representation (ICLR)* (2021).

[44] Jiaming Song, Arash Vahdat, Morteza Mardani, and Jan Kautz. 2023. Pseudoinverse-Guided Diffusion Models for Inverse Problems. In *Proc. International Conference on Learning Representation (ICLR)*.

[45] Jiaming Song, Qinsheng Zhang, Hongxu Yin, Morteza Mardani, Ming-Yu Liu, Jan Kautz, Yongxin Chen, and Arash Vahdat. 2023. Loss-guided diffusion models for plug-and-play controllable generation. In *Proc. International Conference on Machine Learning (ICML)*.

[46] Yang Song, Jascha Sohl-Dickstein, Diederik P Kingma, Abhishek Kumar, Stefano Ermon, and Ben Poole. 2021. Score-Based Generative Modeling through Stochastic Differential Equations. In *Proc. International Conference on Learning Representation (ICLR)*.

[47] Yuhta Takida, Masaaki Imaizumi, Takashi Shibuya, Chieh-Hsin Lai, Toshimitsu Uesaka, Naoki Murata, and Yuki Mitsuishi. 2024. SAN: Inducing Metrizability of GAN with Discriminative Normalized Linear Layer. In *Proc. International Conference on Learning Representation (ICLR)*.

[48] Guy Tevet, Brian Gordon, Amir Hertz, Amit H. Bermano, and Daniel Cohen-Or. 2022. MotionCLIP: Exposing Human Motion Generation to CLIP Space. In *Proc. European Conference on Computer Vision (ECCV)*.

[49] Guy Tevet, Sigal Raab, Brian Gordon, Yoni Shafir, Daniel Cohen-or, and Amit Haim Bermano. 2023. Human Motion Diffusion Model. In *Proc. International Conference on Learning Representation (ICLR)*.

[50] Aäron van den Oord, Oriol Vinyals, and Koray Kavukcuoglu. 2017. Neural discrete representation learning. In *Proc. Advances in Neural Information Processing Systems (NeurIPS)*.

[51] Yin Wang, Zhiying Leng, Frederick WB Li, Shun-Cheng Wu, and Xiaohui Liang. 2023. Fg-t2m: Fine-grained text-driven human motion generation via diffusion model. In *Proc. IEEE/CVF Conference on Computer Vision and Pattern Recognition (CVPR)*.

[52] Yinhuai Wang, Jiwen Yu, and Jian Zhang. 2022. Zero-shot image restoration using denoising diffusion null-space model. *arXiv preprint arXiv:2212.00490* (2022).

[53] Yiming Xie, Varun Jampani, Lei Zhong, Deqing Sun, and Huaiyu Jiang. 2023. Omnicontrol: Control any joint at any time for human motion generation. *arXiv preprint arXiv:2310.08580* (2023).

[54] Jiwen Yu, Yinhuai Wang, Chen Zhao, Bernard Ghanem, and Jian Zhang. 2023. Freedom: Training-free energy-guided conditional diffusion model. In *Proc. IEEE/CVF International Conference on Computer Vision (ICCV)*.

[55] Jiahui Yu, Yuanzhong Xu, Jing Yu Koh, Thang Luong, Gunjan Baid, Zirui Wang, Vijay Vasudevan, Alexander Ku, Yinfai Yang, Burcu Karagol Ayan, Ben Hutchinson, Wei Han, Zarana Parekh, Xin Li, Han Zhang, Jason Baldridge, and Yonghui Wu. 2022. Scaling Autoregressive Models for Content-Rich Text-to-Image Generation. *Transactions on Machine Learning Research* (2022).

[56] Jianrong Zhang, Yangsong Zhang, Xiaodong Cun, Shaoli Huang, Yong Zhang, Hongwei Zhao, Hongtao Lu, and Xi Shen. 2023. T2M-GPT: Generating Human Motion from Textual Descriptions with Discrete Representations. In *Proc. IEEE/CVF Conference on Computer Vision and Pattern Recognition (CVPR)*.

[57] Lvmin Zhang, Anyi Rao, and Maneesh Agrawala. 2023. Adding Conditional Control to Text-to-Image Diffusion Models. In *Proc. IEEE/CVF International Conference on Computer Vision (ICCV)*.

[58] Mingyuan Zhang, Zhongang Cai, Liang Pan, Fangzhou Hong, Xinying Guo, Lei Yang, and Ziwei Liu. 2024. Motiondiffuse: Text-driven human motion generation with diffusion model.

[59] Chongyang Zhong, Lei Hu, Zihao Zhang, and Shihong Xia. 2023. Attt2m: Text-driven human motion generation with multi-perspective attention mechanism. In *Proc. IEEE/CVF Conference on Computer Vision and Pattern Recognition (CVPR)*.

| Notation/Symbol | Description |
|---|--|
| \mathbb{N} | The sets of natural numbers |
| \mathbb{R} | The sets of real numbers |
| \mathbb{R}_+ | The sets of positive real numbers |
| $N \in \mathbb{N}$ | A motion feature dimension |
| $L \in \mathbb{N}$ | A motion length |
| $d_z \in \mathbb{N}$ | A latent space dimension |
| $d_c \in \mathbb{N}$ | A conditional embedding dimension |
| $t \in \mathbb{N}$ | A time step for diffusion model |
| η | A trainable parameter for the encoder |
| ψ | A trainable parameter for the decoder |
| $\phi = \{\varphi, \omega\}$ | A trainable parameter for the discriminator |
| θ | A trainable parameter for the estimator in latent diffusion |
| $x \in \mathbb{R}^{N \times L}$ | A motion input |
| $z \in \mathbb{R}^{d_z}$ | A latent variable |
| $\tau(c) \in \mathbb{R}^{d_c}$ | A output of text encoder corresponding to a prompt c |
| $q_\eta : \mathbb{R}^{N \times L} \rightarrow \mathbb{R}^{d_z} \times \mathbb{R}_+^{d_z}$ | A encoder parameterized by η in Stage 1 |
| $g_\psi : \mathbb{R}^{d_z} \rightarrow \mathbb{R}^{N \times L}$ | A decoder parameterized by ψ in Stage 1 |
| $f_\phi : \mathbb{R}^{N \times L} \rightarrow \mathbb{R}$ | A discriminator parameterized by ϕ in Stage 1 |
| $\epsilon_\theta : \mathbb{R}^{d_z} \times \mathbb{N} \times \mathbb{R}^{d_c} \rightarrow \mathbb{R}^{d_z}$ | A conditional estimator parameterized by θ in Stage 2 |
| $\lambda_{\text{reg}} \in \mathbb{R}_+$ | A weight of VAE regularization term in Stage 1 |
| $\lambda_{\text{adv}} \in \mathbb{R}_+$ | A weight of adversarial loss in Stage 1 |
| $\alpha_t \in (0, 1)$ | A noise scheduling parameter in Stage 2 |
| $\rho_t \in \mathbb{R}_+$ | A time-dependent step size in guided generation |

Table 6: Notation table

A NOTATION

In Table 6, we list the several notations and symbols that we have used in this paper.

B EDITING PROCEDURE ON GUIDED GENERATION

In Algorithm 1, we show the specific procedure for guided generation described in Section 3.4. Note that we apply a time-travel technique to the update rule in Section 3.4 as in [16, 27, 52, 54] to achieve better editing results. This technique adds noise after each gradient descent step to implicitly perform a multi-step optimization of minimizing the distance measuring function $L(\cdot, \mathbf{y})$ and lead to an improvement in the editing quality.

C EVALUATION METRICS DETAILS

We provide more details of evaluation metrics in Section 4.4. We use five metrics to quantitatively evaluate text-to-motion models. These metrics are calculated based on motion and text features extracted with pre-trained networks. More specifically, we utilize the motion encoder and text encoder provided in [14]. We denote ground-truth motion features, generated motion features, and text features as $f_{\text{gt}} = \mathcal{E}_M(x_{\text{gt}}) \in \mathbb{R}^{512}$, $f_{\text{pred}} = \mathcal{E}_M(x_{\text{pred}}) \in \mathbb{R}^{512}$, and $f_{\text{text}} = \mathcal{E}_T(c) \in \mathbb{R}^{512}$, where $\mathcal{E}_M(\cdot)$ and $\mathcal{E}_T(\cdot)$ represent the motion encoder and the text encoder, respectively. We explain the five metrics below.

R-Precision: R-Precision evaluates semantic alignment between input text and generated motion in a sample-wise manner. Given one motion sequence and 32 text descriptions (one ground truth and thirty-one randomly selected mismatched descriptions), we rank the Euclidean distances between the motion and text embeddings. Then, we compute the average accuracy at top-1, top-2, and top-3 places.

Fréchet Inception Distance (FID): FID evaluates the overall motion quality by measuring the distributional difference between

Algorithm 1 Guided Generation for Motion Editing

Require: motion control signal \mathbf{y} , output of text encoder $\tau(c)$, estimator in latent diffusion $\epsilon_\theta(\cdot, t, \tau(c))$, distance measuring function $L(\cdot; \mathbf{y})$, pre-defined parameter $\bar{\alpha}_t$, time-dependent step-size ρ_t , and the repeat times of time-travel of each step $\{r_1, \dots, r_T\}$.

```

1:  $z_T \sim \mathcal{N}(0, I)$ 
2: for  $t = T, \dots, 1$  do
3:   for  $i = r_t, \dots, 1$  do
4:      $\epsilon_t \sim \mathcal{N}(0, I)$ 
5:      $z_{0|t} = \frac{1}{\sqrt{\bar{\alpha}_t}} (z_t - \sqrt{1 - \bar{\alpha}_t} \epsilon_\theta(z_t, t, \tau(c)))$ 
6:      $z_{0|t} = z_{0|t} - \rho_t \nabla_{z_{0|t}} L(g_\psi(z_{0|t}); \mathbf{y})$ 
7:      $z_{t-1} = \sqrt{\bar{\alpha}_t} z_{0|t} + \sqrt{1 - \bar{\alpha}_t - \sigma_t^2} \epsilon_\theta(z_t, t, \tau(c)) + \sigma_t \epsilon_t$ 
8:     if  $i > 1$  then
9:        $\epsilon'_t \sim \mathcal{N}(0, I)$ 
10:       $z_t = \sqrt{\bar{\alpha}_t} z_{t-1} + \sqrt{1 - \bar{\alpha}_t} \epsilon'_t$ 
11:    end if
12:   end for
13: end for
14: return  $g_\psi(z_0)$             $\triangleright$  edited motion generation sample

```

the motion features of the generated motions and those of real motions. We obtain FID by

$$\text{FID} := \|\mu_{\text{gt}} - \mu_{\text{pred}}\|_2^2 - \text{tr}(\Sigma_{\text{gt}} + \Sigma_{\text{pred}} - (2\Sigma_{\text{gt}}\Sigma_{\text{pred}})^{\frac{1}{2}}), \quad (13)$$

where μ_{gt} and μ_{pred} are the mean of f_{gt} and f_{pred} , respectively, Σ_{gt} and Σ_{pred} are their corresponding covariance matrices, and tr denotes the trace of a matrix.

Multi-modal distance (MMDist): MMDist gauges sample-wise semantic alignment between input text and generated motion as well. MMDist is computed as the average Euclidean distance between the motion feature of each generated motion and the text feature of its corresponding description in the test set. Precisely, given N randomly generated samples, it computes the average Euclidean distance between each text feature and its corresponding generated motion feature:

$$\text{MMDist} := \frac{1}{N} \sum_{i=1}^N \|f_{\text{pred},i} - f_{\text{text},i}\|_2^2, \quad (14)$$

where $f_{\text{pred},i}$ and $f_{\text{text},i}$ are the features of the i -th text-motion pair.

Diversity: Diversity measures the variance of the generated motions across the test set. We randomly sample $2S_d$ motions and extract motion features $\{f_{\text{pred},1}, \dots, f_{\text{pred},2S_d}\}$ from the motions. Then, those motion features are grouped into the same size of two subsets, $\{v_1, \dots, v_{S_d}\}$ and $\{v'_1, \dots, v'_{S_d}\}$. The Diversity for this set of motions is defined as

$$\text{Diversity} := \frac{1}{S_d} \sum_{i=1}^{S_d} \|v_i - v'_i\|_2^2. \quad (15)$$

$S_d = 300$ is used in our experiments.

Multi-modality (MModality): MModality measures how much the generated motions diversify within each text description. Given

| Methods | FID \downarrow | R-Precision | Top-1 \uparrow | MMDist \downarrow |
|------------------------|------------------|------------------|------------------|---------------------|
| T2M-GPT [56] | 0.141 \pm .005 | 0.492 \pm .003 | 3.121 \pm .009 | |
| T2M-GPT + GAN (ours) | 0.136 \pm .010 | 0.485 \pm .004 | 3.116 \pm .009 | |
| T2M-GPT + SAN (ours) | 0.133 \pm .006 | 0.494 \pm .003 | 3.111 \pm .013 | |
| MLD [5] | 0.473 \pm .013 | 0.481 \pm .003 | 3.196 \pm .010 | |
| MLD + GAN (ours) | 0.371 \pm .014 | 0.482 \pm .002 | 3.173 \pm .011 | |
| MLD + SAN (MoLA; ours) | 0.362 \pm .009 | 0.514 \pm .003 | 3.162 \pm .008 | |

Table 7: Effectiveness of adversarial training for motion generation performance on HumanML3D

| Methods | FID \downarrow | R-Precision | Top-1 \uparrow | MMDist \downarrow |
|------------------------|------------------|------------------|------------------|---------------------|
| T2M-GPT [56] | 0.514 \pm .029 | 0.416 \pm .006 | 3.007 \pm .029 | |
| T2M-GPT + GAN (ours) | 0.484 \pm .036 | 0.408 \pm .008 | 3.027 \pm .022 | |
| T2M-GPT + SAN (ours) | 0.439 \pm .033 | 0.423 \pm .006 | 2.947 \pm .030 | |
| MLD [5] | 0.404 \pm .027 | 0.390 \pm .008 | 3.204 \pm .027 | |
| MLD + GAN (ours) | 0.382 \pm .028 | 0.385 \pm .005 | 3.305 \pm .035 | |
| MLD + SAN (MoLA; ours) | 0.350 \pm .020 | 0.401 \pm .004 | 3.187 \pm .027 | |

Table 8: Effectiveness of adversarial training for motion generation performance on KIT-ML

a set of motions with K text descriptions, we randomly sample $2S_l$ motions corresponding to the k -th text description and extract motion features $\{f_{\text{pred},k,1}, \dots, f_{\text{pred},k,2S_l}\}$. Then, those motion features are grouped into the same size of two subsets, $\{v_{k,1}, \dots, v_{k,S_l}\}$ and $\{v'_{k,1}, \dots, v'_{k,S_l}\}$. The MModality for this motion set is formalized as

$$\text{MModality} = \frac{1}{K \cdot S_l} \sum_{k=1}^K \sum_{i=1}^{S_l} \|v_{k,i} - v'_{k,i}\|_2^2. \quad (16)$$

$S_l = 10$ is used in our experiments.

D ADDITIONAL EXPERIMENTS FOR MOTION GENERATION

Here, we discuss the effect of adversarial training on Stage 2 to supplement the experiments in Sections 4.3 and 4.4. To demonstrate the broad effectiveness of adversarial training in text-to-motion

generation, we apply adversarial training not only to a continuous latent case as in MLD [5] introduced in Section 3 but also to a discrete latent case as in T2M-GPT [56] introduced in Sections 4.2 and 4.3. The results of two types of methods, (top:) a discrete latent case and (bottom:) a continuous latent case, are shown in Tables 7 and 8. As shown in the tables, our proposed strategy improves existing methods in FID, which is a metric that evaluates the overall motion quality, on both continuous latent and discrete latent cases on both HumanML3D [14] and KIT-ML [36] datasets. Moreover, we can see replacing GAN with SAN boosts performance more on FID, R-precision, and MMDist metrics on both datasets. Note that the only difference between baseline models and our models is training method, not inference, as mentioned in Section 4.4. Therefore, inference with our model can be achieved with equivalent time to MLD and T2M-GPT baselines.